Available online at www.sciencedirect.com
SCIENCE DIRECT
Biochemical and Biophysical Research Communications 341 (2006) 239–244
BBRC
www.elsevier.com/locate/ybbrc

TNP-470 blockage of VEGF synthesis is dependent on MAPK/COX-2 signaling pathway in PDGF-BB-activated hepatic stellate cells ☆

Yan Qing Wang [a,b], John M. Luk [a,*], Andrew C. Chu [a], Kazuo Ikeda [c], Kwan Man [a], Kenji Kaneda [c], Sheung Tat Fan [a,*]

[a] *Center for the Study of Liver Disease, Department of Surgery, The University of Hong Kong, Pokfulam, Hong Kong*
[b] *Liver Transplantation Center of Renji Hospital, Shanghai Second Medical University, Shanghai, China*
[c] *Department of Anatomy, Osaka City University Medical School, Osaka, Japan*

Received 19 December 2005
Available online 9 January 2006

Abstract

Angiogenesis is a key pathogenic event in hepatic fibrogenesis, which is mediated by activated hepatic stellate cells (HSCs). TNP-470 is a known anti-angiogenic agent in cancer, and in this study, we investigated the regulatory mechanisms of TNP-470 blockage of vascular endothelial growth factor (VEGF) synthesis in activated HSCs. Primary HSCs were isolated from rat liver, cultured in vitro, and activated with platelet-derived growth factor-BB (PDGF-BB). After treatment with TNP-470, Nimesulide, PD98059, SB203580 or SP600125, activated HSCs were analyzed by immunoblotting, quantitative RT-PCR, and ELISA for mitogen-activated protein kinase (MAPK) family [ERKs, JNK, and p38], cyclooxygenase-2 (COX-2), and VEGF levels. Phosphorylation of p44/42 MAPK, which was followed by increased expressions of COX-2 and VEGF, was observed in PDGF-BB-activated HSCs; these events could be ameliorated by addition with TNP-470 in time- and dose-dependent manners. TNP-470 also inhibited the secretion of VEGF from activated HSCs into culture supernatant. Furthermore, TNP-470 blockage of VEGF production in activated HSCs could be nullified by exogenous inoculation with prostaglandin E_2. In summary, our findings suggest that TNP-470 exhibits the observed anti-angiogenic properties in activated HSCs by targeting the COX-2/phospho-p44/42 MAPK pathway to inhibit VEGF production.

Keywords: Activated hepatic stellate cells; Angiogenesis; PDGF-BB; VEGF; COX-2; TNP-470

Hepatic stellate cells (HSCs) as tissue-specific pericytes regulate liver homeostasis and play a central role in the response to liver injury [1]. HSCs undergo proliferation and trans-differentiation to myofibroblast-like cells, producing a large number of cytokines and extracellular matrix materials and inducing hepatic fibrosis [2]. HSCs are oxygen sense cells and, in response to exogenous hypoxia or inflammatory environment, they: (i) produce vascular endothelial growth factor (VEGF) protein, (ii) up-regulate the expression of VEGF receptor (VEGFR) protein, and (iii) secrete and deposit extracellular matrix components, particularly type 1 and type III collagens, into the parenchymal region. It is well received that VEGF protein plays a major role in internal metabolism of HSCs and liver fibrogenesis [3,4]. As such, blockage of VEGF production in activated HSCs has drawn intense interest in the treatment of hepatic fibrosis and/or cirrhosis.

Recently, specific neutralizing monoclonal antibodies (R-1mAb and R-2mAb), which inhibit VEGFR-1 and VEGFR-2 significantly, attenuate the development of fibrosis, and are associated with suppression of neovascularization

☆ The study was supported by the CRCG research grant and the Sun Chieh Yeh Research Foundation for Hepatobiliary and Pancreatic Surgery of the University of Hong Kong.
* Corresponding authors. Fax: +852 2819 9636 (J.M. Luk), +852 2818 4407 (S.-T. Fan).
E-mail addresses: jmluk@hkucc.hku.hk (J.M. Luk), hrmsfst@hkucc.hku.hk (S.T. Fan).

0006-291X/$ - see front matter © 2006 Elsevier Inc. All rights reserved.
doi:10.1016/j.bbrc.2005.12.175

in injured liver [5]. Furthermore, tumor-activated HSCs are responsible for deposition of tumor-associated extracellular matrix and creation of proangiogenic microenvironment by secreting VEGF protein as well as basic fibroblast growth factor (bFGF). The despondences are involved in the migration and growth of hepatoma and metastatic cells [6–8]. These findings strongly vouched for the role of VEGF produced by HSCs in causing the fibrogenesis and angiogenesis in liver disease.

Development of new therapeutic strategies that target at the tumor vasculature has aroused an intense interest because angiogenesis is required for the continuing growth of solid tumors [9]. TNP-470 (semisynthetic analogue of fumagillin), as a potent angiogenic inhibitor, targets at methionine aminopeptidase-2 to suppress the growth of tumor and is under clinical trials for anti-cancer therapy [10,11]. The pharmacologic action of TNP-470 is to suppress tumor cells to produce VEGF protein that results in the inhibition of tumor angiogenesis [12,13]. Lower concentration of TNP-470 inhibits the human arterial endothelial cell tube formation by blocking VEGF production from human uterine sarcoma cell line (FU-MMT-1) in a co-cultured model of FU-MMT-1 and human arterial endothelial cells on matrix gel [14]. The events indicate that TNP-470 as an angiogenic inhibitor in part depends on the reduction of VEGF production to attenuate neovascularization.

Despite the angiogenesis inhibition of TNP-470 in cancer being well studied, little is known about its beneficial effects as anti-angiogenic agent in liver fibrogenesis. Our previous study suggested that TNP-470 inhibited the proliferation and activation of hepatic stellate cells [15]. The present work is to further explore the potential signaling molecules targeted by TNP-470 to cause VEGF production blockage in the course of anti-angiogenesis events in PDGF-BB-activated hepatic stellate cells.

Materials and methods

Animals. Specific pathogen-free, male Sprague–Dawley rats (250–300 g) were obtained from the Laboratory Animal Unit of the University of Hong Kong. They were fed on standard chow pellets ad libitum. All the experiments were conducted according to the standard guidelines for animal experiments of the University of Hong Kong.

Isolation and culture of HSCs. HSCs were isolated from the rats as previously reported [15,16]. The cells were suspended in Dulbecco's modified Eagle's medium (DMEM; Gibco Laboratories, Grand Island, NY) with 10% fetal bovine serum (FBS; Gibco Laboratories) in the cell density of 5×10^5 cells/ml with penicillin-and-streptomycin antibiotics. The purity of HSCs was higher than 95% and the viability was over 90% as in previous reports. Activated HSCs were obtained after a 1-week culture of freshly isolated HSCs in the dishes with 10% FBS–DMEM and were used after starvation for 24 h with 0.5% FBS–DMEM. They were then incubated by 10 ng/ml PDGF-BB or 10 μmol PGE_2 for 0.25, 0.5, 3, 6, 9, and 12 h with, or without, the pretreatment of 0.1, 1, and 10 μg/ml TNP-470 (a kind gift from Takeda Pharmaceutical Industries, Osaka, Japan), 12 μmol/ml PD98059 (sc-3532; Santa Cruz Biotechnology, Santa Cruz, CA), 100 μmol Nimesulide (Sigma Chemical, St. Louis, MO), 10 μmol SB203580 (sc-3533; Santa Cruz Biotechnology) or 50 μmol SP600125 (Sigma Chemical) for 0.5 h in serum-free medium.

Western blot analysis. The activity of mitogen-activated protein kinase (MAPK) was measured using the MAPK assay kit (Cell Signaling Technology, Beverly, MA) according to the manufacturer's protocol. Sodium dodecyl sulfate (SDS) sample buffer (62.5 mM Tris–HCl [pH 6.8 at 25 °C], 2% w/v SDS, 10% glycerol, 50 mM DTT, and 0.01% bromophenol blue) was added to the culture dishes. Immediately, the cells were scraped off the plate, and the extract was transferred to a micro-centrifuge tube and kept on ice. Samples were denatured at 95 °C for 5 min after 10–15 s sonication. The protein concentration was determined by Bradford's method, respectively. The samples of 30 μg protein were fractionated on 10% SDS–PAGE and transferred to polyvinylidene difluoride membranes. After washing, the membrane was treated with 5% skim milk at room temperature for 1 h and incubated with mouse monoclonal antibody against β-actin (1:5000 dilution; Sigma-Aldrich, St. Louis, MO) and p-JNK (clone G7) (1:1000 dilution; Santa Cruz Biotechnology), rabbit polyclonal antibodies against cyclooxygenase-2 (COX-2) (1:1000 dilution; Santa Cruz Biotechnology), VEGF (1:1000 dilution; Santa Cruz Biotechnology), and p38 (1:1000 dilution; Santa Cruz Biotechnology), rabbit polyclonal antibody against phospho-p44/42 MAPK (1:1000 dilution; Cell Signaling Technology), and p44/42 MAPK (1:1000 dilution; Cell Signaling Technology), respectively, at 4 °C overnight. For the secondary antibodies, they were horseradish peroxidase-conjugated anti-rabbit antibodies (1:2000 dilution; Dako, Carpinteria, CA) for VEGF, COX-2, p38, phospho-p44/42 MAPK, and p44/42 MAPK or anti-mouse antibodies for β-actin and p-JNK (G-7), and incubated with the membrane at room temperature for 1 h. After extensive washing with Tris-buffered saline/Tween 20 (1%), the immunoreactive bands were visualized on an X-ray film by ECL detection (Amersham Bioscience, Arlington Heights, IL). The density of bands was quantitated with a laser densitometer (ATTO densitograph 4.0, Atto, Tokyo, Japan), and the mean value was calculated from three independent experiments.

Real-time quantitative reverse transcription (RT)-polymerase chain reaction (PCR). Total RNA was extracted using RNeasy Midi Kit (QIAGEN Company GmbH, Germany) and the quality of the total RNA was detected by spectrophotometer (DU-65, Beckman Coulter, Fullerton, CA). About 1 μg total RNA from each sample was used to perform RT reaction. TaqMan Reverse Transcription Reagents (Applied Biosystems, Foster City, CA) were used according to the manufacturer's instruction (25 °C × 10 min, 48 °C × 30 min, and 95 °C × 5 min). RT product (1 μl) was used to perform real-time quantitative PCR with a reaction volume of 50 μl (TaqMan Q-PCR Core Reagent Kit, Applied Biosystems) by ABI PRISM7700 Sequence Detection System (Applied Biosystems). Probes and primers of VEGF were designed under the Primer Express software according to the criteria for real-time PCR (Applied Biosystems). The sequences of the primer were VEGF(S) (5′-AGCGGA GAAAGC ATT TGT TTG-3′) and VEGF (AS) (5′-CAACGC GAGTCT GTTTTG-3′), and the probe was 5′-CCAAGA TCCGCA GACGTG TAAATG TTCC-3′. The TaqMan Ribosomal RNA Control Reagent (18 S RNA probe [VIC] and primers; Applied Biosystems) was used for internal control in the same PCR plate well to normalize the target gene amplification copies. The PCR protocol was in accordance with the manufacturer's recommendation (50 °C × 2 min, 95 °C × 10 min, and [95 °C × 15 s, 60 °C × 1 min] × 50 cycles). All samples were detected in triplicate and the reading from each sample and its internal control was used to calculate gene expression levels. After normalization with the internal control, gene expression levels after reperfusion were calculated as the percentage of the basal levels before graft harvesting.

Enzyme-linked immunosorbent assay (ELISA). Isolated HSCs were cultured in 6-well plates at a density of 5×10^5 cells per well for 1 week with 10% FBS–DMEM. The medium was changed for starvation with 0.5% FBS–DMEM for 24 h and removed. The starved HSC cells were treated by PDGF-BB (10 ng/ml) for 3, 6, 9, and 12 h with or without the pretreatment of 0.1, 1, and 10 μg/ml TNP-470 for 0.5 h in serum-free medium. The supernatants were collected, respectively. After high-speed centrifugation to remove cellular debris, the amount of VEGF in the supernatants was measured by the colorimetric VEGF ELISA using 96-well microplate coated with polyclonal antibody specific for mouse $VEGF_{164}$ (R&D Systems, Minneapolis, MN).

Statistics. Data were represented by means ± standard error of means. Comparison of the effects of various treatments was performed with one-way ANOVA and a two-tailed t test. P values of less than 0.05 were considered statistically significant.

Results

TNP-470 inhibits pro-angiogenic events in activated HSCs

PDGF-BB was the most potent mitogen for HSCs in culture. Binding of PDGF to PDGF receptor-β recruited a signaling molecule Ras leading to MAPK cascades and sequentially produced some cytokines to modulate metabolism homeostasis in HSCs [1]. Because our previous study demonstrated that TNP-470 blocked PDGF receptor-β to inhibit HSC proliferation and activation [15], we thus examined the inhibitory effect of TNP-470 on the MAPK-dependent (p44/42 MAPK, JNK, and p38) signaling pathway and the downstream target COX-2 and VEGF molecules in the PDGF-BB-stimulated HSCs. As shown by Western blot (Fig. 1), HSCs were activated by PDGF-BB to induce (i) phosphorylation of MAP kinases (ERK1 peaks at 0.25 and 3 h, and p42 at 0.5 h), and JNK and p38 MAP kinase (peak at 0.5 h), followed by slow declination; (ii) increased expression of COX-2 (peak at 3 h) and VEGF (peak at 6 h). Pretreatment of the PDDF-BB-stimulated HSCs with anti-angiogenic inhibitor TNP-470 was demonstrated to suppress the phosphorylation of p44/42 MAPK (total p44/42 MAPK proteins remained constant) and reduce the expression of phosphorylated JNK as revealed by G7 antibody which recognized phosphorylated Thr-183 and Tyr-185 residues. On the contrary, there was no apparent effect on p38 MAPK. Blockage of the described signaling events for VEGF production was observed in a dose- and time-dependent manner with TNP-470 treatment (Figs. 1A and B).

Down-regulated expression and secretion of VEGF isoforms by TNP-470

As shown by real-time RT-PCR (Fig. 2A), PDGF-BB (10 ng/ml) remarkably upregulated the VEGF mRNA transcription by about 800-fold at 6 h in activated HSCs that could be inhibited by TNP-470 treatment in a dose-de-

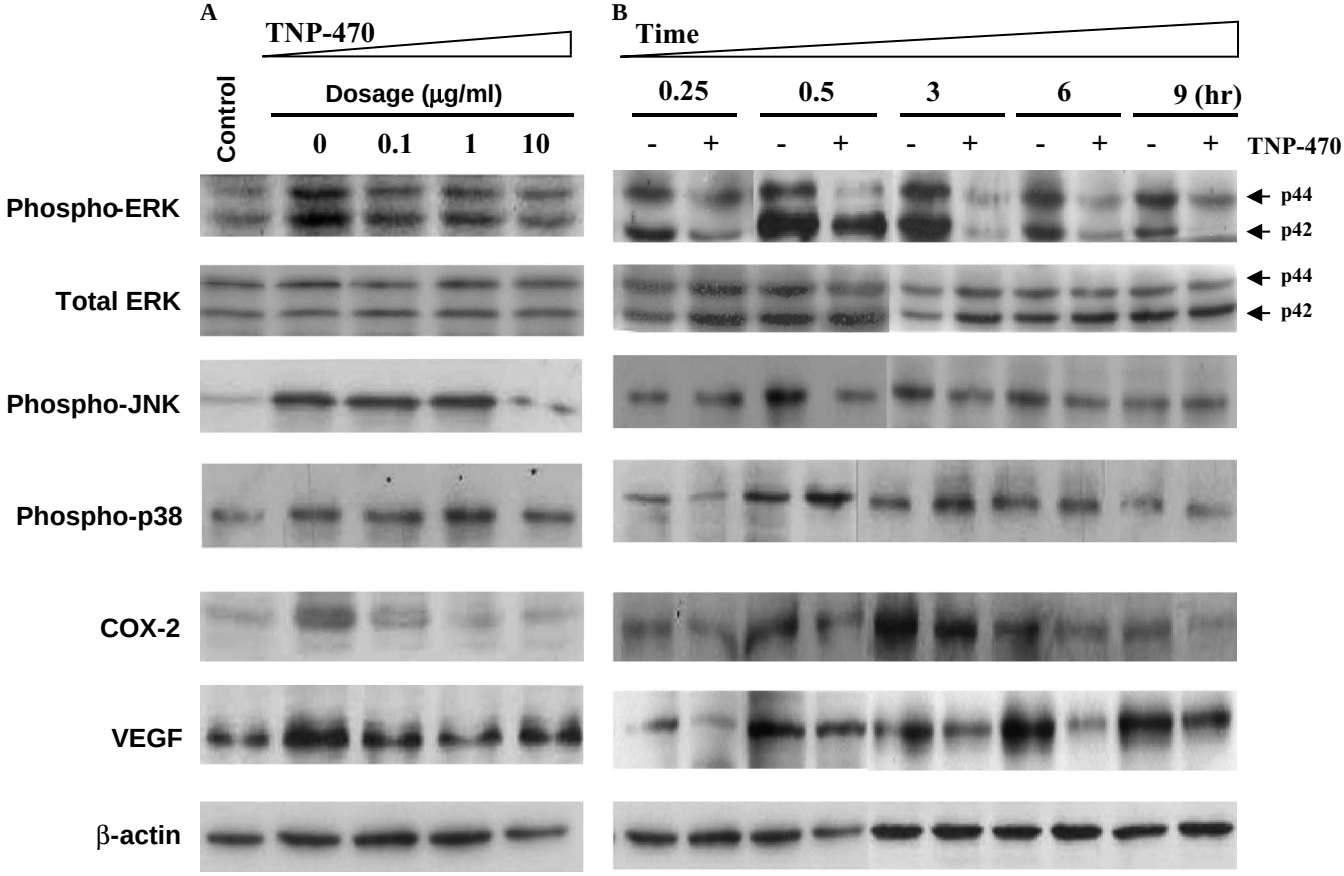

Fig. 1. Immunoblotting analysis of VEGF and MAPK/COX-2 proteins in PDGF-BB-activated HSCs with or without TNP-470 treatment. (A) Primary HSCs were activated by PDGF-BB (10 ng/ml) for 6 h with 30-min pretreatment of TNP-470 at increasing dosages (0.1, 1 or 10 μg/ml). HSCs without any PDGF stimulation or TNP-470 treatment were used as the baseline control. Cell lysates were subjected to SDS–PAGE and probed with the following antibodies specific for the phosphorylated forms of p44/42 MAPK, JNK, and p38; total p44/p42 MAPK, COX-2, and VEGF proteins. β-Actin immunoblot was included as the internal loading control. (B) Primary HSCs were activated by PDGF-BB (10 ng/ml) with (+), or without (−), 30-min pretreatment of TNP-470 (10 μg/ml) for designated time intervals (0.25, 0.5, 3, 6, and 9 h). Immunoblotting was similarly performed as described above in (A). All experiments were conducted in triplicate and representative figures were shown.

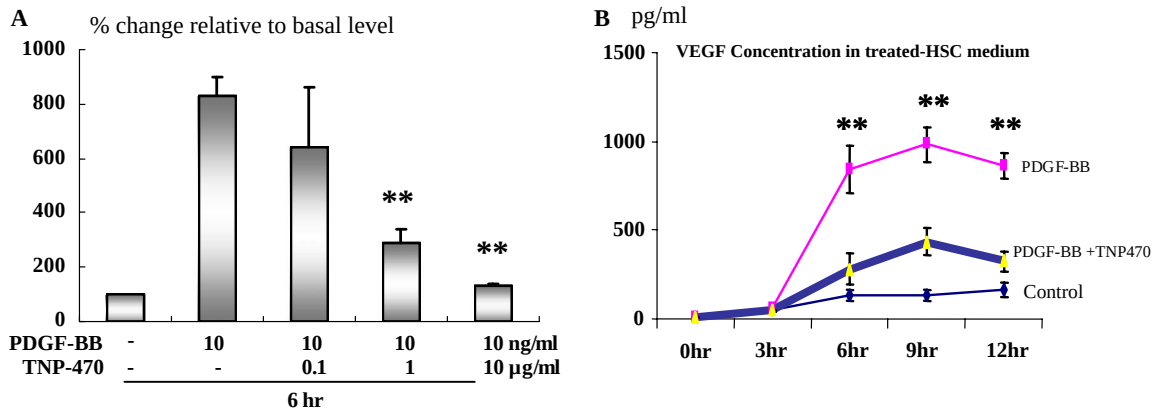

Fig. 2. TNP-470 inhibited the synthesis of $VEGF_{165}$ in PDGF-BB-activated HSCs. (A) TaqMAN real-time quantitative RT-PCR analysis of $VEGF_{165}$ mRNA level from PDGF-BB-activated HSCs, with or without pretreatment of TNP-470 at increasing dosages (0.1, 1, and 10 μg/ml). HSCs without any PDGF stimulation or TNP-470 treatment were used as the baseline control. Data are presented as means ± SEM. $n = 3$, $^{**}P \leqslant 0.01$ vs. treatment with 10 ng/ml PDGF for 6 h. (B) TNP-470 reduced VEGF secretion from PDGF-BB-activated HSCs. $VEGF_{165}$ concentration was measured by ELISA in HSC culture medium at designated time intervals: 3, 6, 9 or 12 h. *PDGF-BB*, HSC was stimulated with 10 ng/ml PDGF-BB; *PDGF-BB + TNP470*, PDGF-BB-activated HSC was pretreated with 10 μg/ml TNP-470 for 30 min; *Control*, HSC culture without any PDGF stimulation or TNP-470 treatment. Data are presented as means ± SEM. $n = 3$, $^{**}P \leqslant 0.01$ vs. with PDGF-BB treatment only.

pendent manner. Fig. 2B demonstrates the VEGF protein level in culture medium as determined by ELISA. The VEGF protein was detectable in culture medium obtained from PDGF-BB-activation HSCs after 6-h incubation, and the level remained at about 800–1000 pg/ml until 12 h. Again, pretreatment with TNP-470 (10 μg/ml) could significantly attenuate the VEGF secretion from the activated HSCs in cultures ($P < 0.05$, $n = 3$).

TNP-470 blockage of VEGF synthesis was dependent on COX-2 and p44/42-MAPK signaling in activated HSCs

To investigate the signaling pathway of COX-2 and MAPK kinases involved in VEGF production in activated HSCs, we employed a panel of specific pharmacological inhibitors in the study (Fig. 3A): Nimesulide (COX-2-specific inhibitor), PD98059 (selective inhibitor of MAPK kinase),

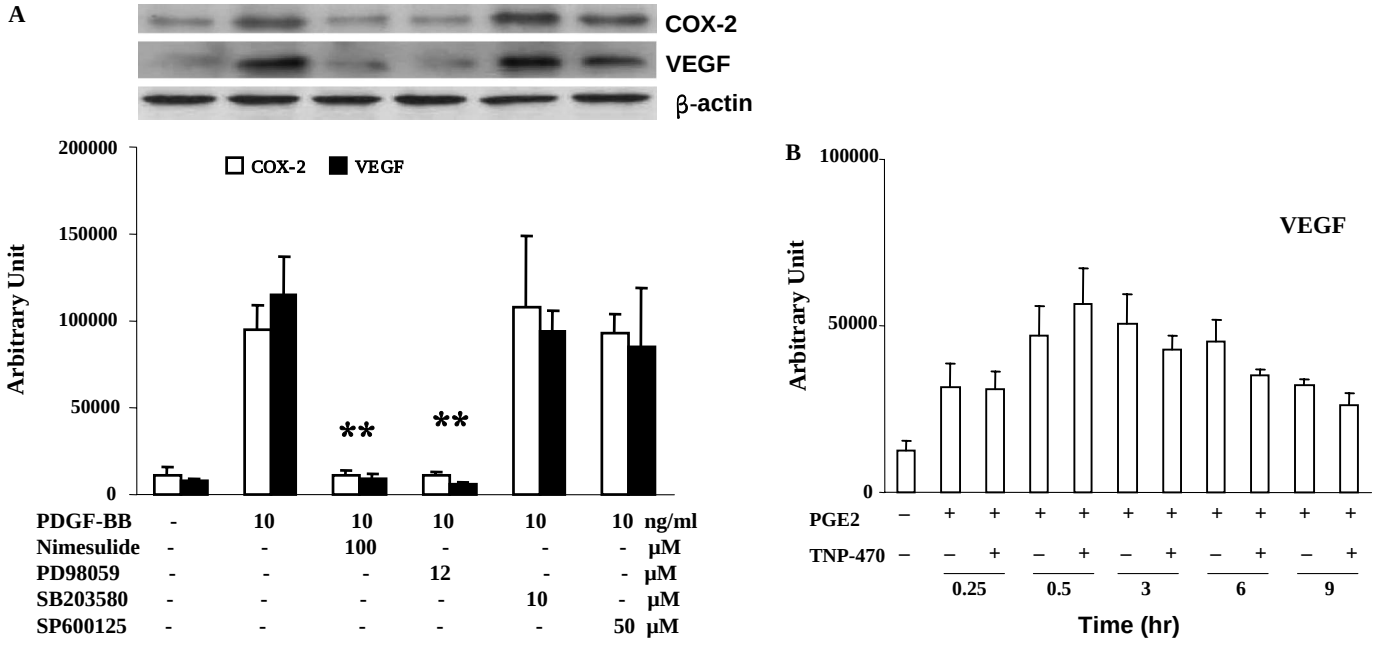

Fig. 3. VEGF synthesis depends on COX-2/PGE_2 expression via phospho-p44/42 MAPK cascade signal in activated HSCs. (A) Immunoblot analyses for COX-2 and VEGF proteins in PDGF-BB-activated HSCs for 3 h with the following pretreatment: Nimesulide (100 μM), PD98059 (12 μM), SB203580 (10 μM) or SP600125 (10 μM). The compounds were solubilized in serum-free Dulbecco's modified Eagle's medium and incubated with cultures for 30 min. Data are presented as means ± SEM. $n = 3$, $^{**}P \leqslant 0.01$ vs. with PDGF-BB treatment only. β-Actin was included as internal loading control. (B) Exogenous PGE_2 rescues the VEGF production in TNP-470-treated HSCs. Immunoblot analyses of VEGF protein in PDGF-activated HSCs following exogenous inoculation of PGE_2 (10 μM) for specified time intervals (0.25, 0.5, 3, 6, and 9 h), with (+) or without (−) the pretreatment of 10 μg/ml TNP-470 for 30 min in serum-free Dulbecco's modified Eagle's medium. Data are presented as means ± SEM. $n = 3$ vs. treatment with 10 ng/ml PDGF-BB and 10 μmol PGE_2, respectively.

SB203580 (a selective pharmacologic inhibitor of p38 MAPK), and SP600125 (selective inhibitor of JNK). Among them, only the Nimesulide and PD98059 compounds were able to suppress the COX-2 and VEGF expression in the PDGF-BB-activated HSCs. These results suggested that COX-2 was the downstream target of phosphorylation of p44/42 MAPK for VEGF production in activated HSCs under the stimulation of PDGF signal transduction. On the other hand, the JNK and p38 inhibitors did not demonstrate the similar inhibitory effects on VEGF and/or COX-2 expression, and p-JNK and p38 MAPK signals were not involved in COX-2/MAPK signaling cascade leading to VEGF production in PDGF-BB-activated HSCs.

These COX-2-dependent inhibitory events could be superseded by exogenous inoculation of PGE_2, and VEGF production was rapidly rescued (peak at 3 h) in a time-dependent manner (Fig. 3B). Despite pretreatment with TNP-470, there was no apparent inhibitory effect on the production of VEGF proteins. In short, COX-2 was the downstream target of TNP-470 via phosphorylation of p44/42 MAPK signaling to initiate its anti-angiogenic properties in activated HSCs.

Discussion

During liver injury, HSCs were activated to increase surface expression of PDGF receptors. Upon PDGF stimulation, the PDGF receptors were dimerized and RasG protein was being recruited to initiate downstream signaling events for cell proliferation and differentiation activities [1]. Our present findings demonstrated that: (i) the growth factor PDGF-BB also induced VEGF production in activated HSCs and secretion to the surrounding medium, (ii) the PDGFR-mediated VEGF production pathway was dependent on the phosphorylation of p44/42 MAPK kinase and COX-2 expression, and (iii) exogenous prostaglandin PGE_2 could directly activate the VEGF production without the requirement of PDGF-mediated signaling. In our previous report, the COX-2 is required to catalyze arachidonic acid for the synthesis of PGE_2, and subsequently induce the expression of hypoxia-inducible factor-1α that leads to the degradation of von Hippel–Lindua protein, a negative regulator of VEGF production [17]. Therefore, it is believed that the PDGF-BB induces the VEGF synthesis in activated HSCs is dependent on the MAPK-COX-2 signaling pathway.

To further examine this hypothesis, we employed TNP-470 (a known angiogenic inhibitor in cancer) to inhibit VEGF production in PDGF-activated HSCs and to determine whether it was mediated through the phosphorylation of p44/42 MAPK and increased expression of COX-2 protein. Our data clearly supported this model, and the inhibitory effects of TNP-470 could be reversed or rescued by addition of exogenous PGE_2, which is the downstream substrate of COX-2 target. Therefore, the inhibitory effect of TNP-470 on VEGF production attributes to the blockade of MAPK/COX-2 signaling pathway in activated HSCs.

Initially, TNP-470 is proved to be an effective anti-tumor agent in both the in vitro and animal models, and is currently in phase III clinical trials [10,18–20]. Further studies have also shown that TNP-470 is even better to suppress tumor growth when combined with conventional chemotherapy [21,22]. Attributing to its anti-angiogenic effect, TNP-470 inhibits endothelial cell proliferation in the process of angiogenesis, thereby reducing the synthesis of proangiogenic factors in tumor microenvironment, such as VEGF and bFGF proteins [13,14,20]. In addition, it could also suppress the formation of lymphatic capillaries around the tumor (i.e., lymphangiogenesis) and attenuate the proliferation of fibroblast cells [23].

In liver fibrogenesis, activated HSCs secrete interleukin-8, bFGF, and VEGF to promote endothelial cell growth and proliferation [8,18]. In our earlier study, TNP-470 was shown to suppress the progression of hepatic fibrosis in vitro. Proliferation and activation of HSCs were remarkably subdued, probably by blocking PDGF receptor-β signaling and cyclin D_1/cdk_4 cell cycle arrest. We also demonstrated that TNP-470 inhibited angiogenesis derived from hypoxic tissue injury by CCl_4-induced hepatic fibrosis model [15].

Herein, pretreatment of TNP-470 in activated HSCs reduced the phospho-p44/p42 MAPK activity and COX-2 expression preceding the production of VEGF derived from the PDGF-BB-mediated signaling pathway. Likewise, treatment with PD98059 (MAPK inhibitor) also suppressed the production of VEGF and COX-2 protein in PDGF-activated HSCs, implying the involvement of MAPK-COX-2 signaling axis. We next examined the inhibitory effect of Nimesulide (COX-2 inhibitor) on VEGF expression under hypoxia and PDGF-BB stimulation in activated HSCs. Our studies strongly supported the fact that COX-2 could up-regulate the production of VEGF derived from activated HSCs. Another piece of evidence is demonstrated by exogenous PGE_2 that could nullify the inhibitory effect of TNP-470 and rescue the VEGF production in PDGF-activated HSCs.

Evidently, p44/p42 MAPK plays a crucial role in regulating the pro-angiogenic process by (i) activation and phosphorylation of cytosolic phospholipase A2 in arachidonic acid metabolism [24] and/or (ii) having direct impact on Sp1 transcriptional activity to enhance VEGF synthesis [25]. Thus, TNP-470 blockage of the MAPK/COX-2 signaling cascade in PDGF-activated HSCs may result in attenuation of the angiogenesis during liver fibrogenic events.

Acknowledgment

The authors thank Dr. Katsuichi Sudo (Takeda Chemical Industries, Osaka, Japan) for providing TNP-470.

References

[1] D. Li, S.L. Friedman, Hepatic stellate cells: morphology, function, and regulation, in: I.M. Arais (Ed.), The Liver: Biology and Pathobiology, fourth ed., Raven Press, New York, 2001, pp. 455–468.

[2] A.M. Rappaport, P.J. MacPhee, M.M. Fisher, M.J. Phillips, The scarring of the liver acini (Cirrhosis). Tridimensional and microcirculatory considerations, Virchows. Arch. A. Pathol. Anat. Histopathol. 402 (1983) 107–137.

[3] V. Ankoma-Sey, M. Matli, K.B. Chang, A. Lalazar, D.B. Donner, L. Wong, R.S. Warren, S.L. Friedman, Coordinated induction of VEGF receptors in mesenchymal cell types during rat hepatic wound healing, Oncogene 17 (1998) 115–121.

[4] C. Corpechot, V. Barbu, D. Wendum, N. Kinnman, C. Rey, R. Poupon, C. Housset, O. Rosmorduc, Hypoxia-induced VEGF and collagen I expressions are associated with angiogenesis and fibrogenesis in experimental cirrhosis, Hepatology 35 (2002) 1010–1021.

[5] H. Yoshiji, S. Kuriyama, J. Yoshii, Y. Ikenaka, R. Noguchi, D.J. Hicklin, Y. Wu, K. Yanase, T. Namisaki, M. Yamazaki, H. Tsujinoue, H. Imazu, T. Masaki, H. Fukui, Vascular endothelial growth factor and receptor interaction is a prerequisite for murine hepatic fibrogenesis, Gut 52 (2003) 1347–1354.

[6] E. Olaso, C. Salado, E. Egilegor, V. Gutierrez, A. Santisteban, P. Sancho-Bru, S.L. Friedman, F. Vidal-Vanaclocha, Proangiogenic role of tumor-activated hepatic stellate cells in experimental melanoma metastasis, Hepatology 37 (2003) 674–685.

[7] O.N. El-Assal, A. Yamanoi, Y. Soda, M. Yamaguchi, M. Igarashi, A. Yamamoto, T. Nabika, N. Nagasue, Clinical significance of microvessel density and vascular endothelial growth factor expression in hepatocellular carcinoma and surrounding liver: possible involvement of vascular endothelial growth factor in the angiogenesis of cirrhotic liver, Hepatology 27 (1998) 1554–1562.

[8] J.O. Jung, G.Y. Gwak, Y.S. Lim, C.Y. Kim, H.S. Lee, Role of hepatic stellate cells in the angiogenesis of hepatoma (in Korean), Korean J. Gastroenterol. 42 (2003) 142–148.

[9] T.M. Niederman, Z. Ghogawala, B.S. Carter, H.S. Tompkins, M.M. Russell, R.C. Mulligan, Antitumor activity of cytotoxic T lymphocytes engineered to target vascular endothelial growth factor receptors, Proc. Natl. Acad. Sci. USA 99 (2002) 7009–7014.

[10] N. Sin, L. Meng, M.Q. Wang, J.J. Wen, W.G. Bornmann, C.M. Crews, The anti-angiogenic agent fumagillin covalently binds and inhibits the methionine aminopeptidase, MetAP-2, Proc. Natl. Acad. Sci. USA 94 (1997) 6099–6103.

[11] C.M. Brdlik, C.M. Crews, A single amino acid residue defines the difference in ovalicin sensitivity between type I and II methionine aminopeptidases, J. Biol. Chem. 279 (2004) 9475–9480.

[12] M. Toi, T. Ueno, T. Tominaga, New molecular target of cancer therapy-angiogenesis regulator VEGF (in Japanese), Gan To Kagaku Ryoho 24 (1997) 2202–2206.

[13] S.M. Rybak, E. Sanovich, M.G. Hollingshead, S.D. Borgel, D.L. Newton, G. Melillo, D. Kong, G. Kaur, E.A. Sausville, "Vasocrine" formation of tumor cell-lined vascular spaces: implications for rational design of anti-angiogenic therapies, Cancer Res. 63 (2003) 2812–2819.

[14] S. Miura, M. Emoto, Y. Matsuo, T. Kawarabayashi, K. Saku, Carcinosarcoma-induced endothelial cells tube formation through KDR/Flk-1 is blocked by TNP-470, Cancer Lett. 203 (2004) 45–50.

[15] Y.Q. Wang, K. Ikeda, T. Ikebe, K. Hirakawa, M. Sowa, K. Nakatani, N. Kawada, K. Kaneda, Inhibition of hepatic stellate cell proliferation and activation by the semisynthetic analogue of fumagillin TNP-470 in rats, Hepatology 32 (2000) 980–989.

[16] K. Ikeda, T. Wakahara, Y.Q. Wang, H. Kadoya, N. Kawada, K. Kaneda, In vitro migratory potential of rat quiescent hepatic stellate cells and its augmentation by cell activation, Hepatology 29 (1999) 1760–1767.

[17] Y.Q. Wang, J.M. Luk, K. Ikeda, K. Man, A.C. Chu, K. Kaneda, S.T. Fan, Regulatory role of vHL/HIF-1α in hypoxia-induced VEGF production in hepatic stellate cells, Biochem. Biophys. Res. Commun. 317 (2004) 358–362.

[18] K. Inoue, M. Chikazawa, S. Fukata, C. Yoshikawa, T. Shuin, Frequent administration of angiogenesis inhibitor TNP-470 (AGM-1470) at an optimal biological dose inhibits tumor growth and metastasis of metastatic human transitional cell carcinoma in the urinary bladder, Clin. Cancer Res. 8 (2002) 2389–2398.

[19] Z.M. Bhujwalla, D. Artemov, K. Natarajan, M. Solaiyappan, P. Kollars, P.E. Kristjansen, Reduction of vascular and permeable regions in solid tumors detected by macromolecular contrast magnetic resonance imaging after treatment with antiangiogenic agent TNP-470, Clin. Cancer Res. 9 (2003) 355–362.

[20] A. Pourtier-Manzanedo, C. Vercamer, E. Van Belle, V. Mattot, F. Mouquet, B. Vandenbunder, Expression of as Ets-1 dominant-negative mutant perturbs normal and tumor angiogenesis in a mouse ear model, Oncogene 22 (2003) 1795–1806.

[21] R.S. Herbst, T.L. Madden, H.L. Tran, G.R. Blumenschein Jr., C.A. Meyers, L.F. Seabrooke, F.R. Khuri, V.K. Puduvalli, V. Allgood, H.A. Fritsche Jr., L. Hinton, R.A. Newman, E.A. Crane, F.V. Fossella, M. Dordal, T. Goodin, W.K. Hong, Safety and pharmacokinetic effects of TNP-470, an angiogenesis inhibitor, combined with paclitaxel in patients with solid tumors: evidence for activity in non-small-cell lung cancer, J. Clin. Oncol. 20 (2002) 4440–4447.

[22] E.S. Kim, R.S. Herbst, Angiogenesis inhibitors in lung cancer, Curr. Oncol. Rep. 4 (2002) 325–333.

[23] R. Satchi-Fainaro, M. Puder, J.W. Davies, H.T. Tran, D.A. Sampson, A.K. Greene, G. Corfas, J. Folkman, Targeting angiogenesis with a conjugate of HPMA copolymer and TNP-470, Nat. Med. 10 (2004) 255–261.

[24] L.L. Lin, M. Wartmann, A.Y. Lin, J.L. Knopf, A. Seth, R.J. Davis, cPLA2 is phosphorylated and activated by MAP kinase, Cell 72 (1993) 269–278.

[25] J. Milanini-Mongiat, J. Pouyssegur, G. Pages, Identification of two Sp1 phosphorylation sites for p42/p44 mitogen-activated protein kinases: their implication in vascular endothelial growth factor gene transcription, J. Biol. Chem. 277 (2002) 20631–20639.